Trabecular bone scaffolding using a biomimetic approach

T. VAN CLEYNENBREUGEL, H. VAN OOSTERWYCK, J. VANDER SLOTEN
Division of Biomechanics and Engineering Design, K.U. Leuven, Celestijnenlaan 200A, 3001-Leuven, Belgium

J. SCHROOTEN
Department of Metallurgy and Materials Engineering, K.U. Leuven, Kasteelpark Arenberg 44, 3001-Leuven, Belgium
E-mail: tvc@mech.kuleuven.ac.be

The current treatment of large bone defects has several disadvantages. An alternative for using grafts or bone cement for the filling of bone cavities is the use of a bone scaffold that provides a temporary load-bearing function. This paper describes a biomechanical design procedure for a personalized implant with a geometry that has a good fit inside the defect and an internal architecture that provides a scaffold with optimized mechanical properties. These properties are optimized for a load-bearing application, for avoiding stress shielding in the bone surrounding the implant and for activation of osteoblasts seeded inside the scaffold. The design is based on medical images both of the defect and of healthy bone tissue that is representative for the tissue being replaced by the scaffold. Evaluation of the scaffold's mechanical properties is done with high-resolution finite element analyzes of the scaffold and healthy bone. This allows matching of the scaffold and bone mechanical properties, thus giving the scaffold its biomimetic properties.

1. Introduction

This paper concentrates on the treatment of one specific type of bone defect: the cavities resulting from the removal of benign bone tumors. The treatment of benign tumors consists typically of a removal of the tumor and a consequent filling of the cavity, using either bone cement polymethyl-metacrylate (PMMA) or a bone graft [1]. However, both treatments have their disadvantages. PMMA is not resorbable, therefore it does not allow new bone formation in the cavity. An autograft, which is still the ''gold standard'' for treatment of bone defects, has a limited availability and is therefore only suitable for small defects [2]. Moreover, a graft does not provide a strength restoration of the affected limb, hence no early loading is allowed.

In recent years a strong tendency is noticeable towards regeneration of bone defects, hence creation of tissue identical to that lost or injured [3]. Most research in the regeneration of bone tissue is concentrating on structures (''bone scaffolds'') that are used to fill the defect, stimulate new bone formation and that are resorbed over time and replaced by newly formed bone [3]. It is important that the mechanical properties of the scaffold are well defined and controlled, as is demonstrated by following arguments:

- The load-bearing scaffold should carry the loads imposed during daily activity without collapsing so that early function restoration is obtained. Early loading of the affected limb will substantially improve the patient's quality of life.
- It has been reported in literature that mechanical loading of bone tissue is needed in order to maintain or increase the amount of bone tissue present [4, 5]. This has important implications on the scaffold design at several levels:
  - Bone cells grown inside the porous scaffold should feel sufficient mechanical loading so that they are stimulated to form new bone.
  - Stress shielding should be avoided in the bone surrounding the scaffold. Therefore the scaffold stiffness should be kept sufficiently low compared to the surrounding bone.
  - New bone that has grown from the surroundings into the scaffold surface should be deformed enough to stimulate further bone formation and bone growth inside the scaffold.

From this it is clear that there is a need for the bone scaffold to have the appropriate mechanical properties. This paper describes the biomechanical design of a bone scaffold for the regeneration of trabecular bone tissue. The design procedure uses a biomimetic approach: the mechanical properties of the scaffold are matched to those of the healthy bone surrounding the defect.

2. Materials and methods

A biomimetic bone scaffold is obtained by adapting the mechanical properties of the scaffold to match those of healthy trabecular bone. Comparison of the mechanical properties of the scaffold with those of the healthy bone is obtained using high-resolution finite element models of both structures. The complete designing process can be divided into two steps:

1. Generation of the numerical models of bone tissue and scaffold.
2. Assessment and comparison of the mechanical properties of both models.

If the mechanical properties of the scaffold are not sufficiently mimicking those of the healthy bone tissue then a new iteration step is needed until a satisfying result is obtained. For both steps the materials and methods will be discussed in greater detail.

2.1. Model generation

2.1.1. Bone model

Since trabecular bone differs from one individual to another, and from one location to another within one individual, it would be favorable if the scaffold properties were individually adjusted to the patient and to the location of the defect. This is realized by acquiring high-resolution images of healthy bone tissue that is representative for the bone that will be replaced by the scaffold. This can be bone adjacent to the defect, or from the contralateral side if the defect is unilateral. The imaging modalities used can be peripheral quantitative computed tomography (pQCT) [6] or micro magnetic resonance-imaging (μMRI) [7]. Both are already *in vivo* applicable and provide images of sufficiently high resolution. In the future micro computed tomography (μCT) can be an option when the radiation dose can be sufficiently reduced.

From these images a high-resolution finite element model of healthy bone tissue of the patient is generated. This is done using software routines, written in Matlab 6.1 (The MathWorks, Inc): the image set is converted to a 3D-matrix of grey values representing the attenuation properties of each volume element (voxel), a threshold value is selected separating the bone voxels from the soft tissue voxels and each bone voxel is converted into a cube-shaped element with eight nodes. This set of elements and nodes is then imported into Mentat 2001 (MSC Software) for further analysis.

2.1.2. Scaffold model

The scaffold is designed at two levels: the outer geometry and the internal architecture. The scaffold must have an outer geometry that ensures a good fit inside the defect. Therefore the shape of the scaffold is based on clinical CT-images of the bone defect. This is done in the software Mimics (Materialise) and involves the pre-operative planning, performed by the surgeon who determines which part of the bone will be removed during surgery. The obtained 3D-shape of the defect is then exported to a neutral file format (IGES) and imported to the computer-aided design (CAD)-environment AutoCad 2002 (Autodesk) and used for the design of the outer shape of the scaffold. The internal architecture of the scaffold is created using boolean substraction of the desired shape of the pores from the outer geometry of the scaffold. A similar approach has been used by Hollister *et al*. [8]. The resulting structure is imported in Mentat 2001, where the geometry is meshed using the algorithms of Mentat. The final result is a tetrahedron or hexahedron mesh of the scaffold structure.

2.2. Mechanical evaluation

The bone model and scaffold model are subjected to the simulation of a mechanical compression test that allows assessment of the mechanical properties of both. First, the material properties of the bone model and scaffold model are assigned and the appropriate boundary conditions are imposed on the models: for a compression test a vertical displacement is applied to the top surface, while the vertical displacement is restrained at the bottom surface. Then the analysis is performed. Finally, the mechanical properties are compared. For evaluation of the biomimetic ability of the scaffold two parameters are calculated for the scaffold model and the bone model:

(1) The apparent stiffness of the structure is calculated from the reaction forces at the bottom surface of the model, using following formula:

$$E = \frac{\sum F_i}{A} \cdot \frac{1}{\varepsilon}$$

with $\sum F_i$ being the sum of the reaction forces over the bottom surface of the model; A the cross-sectional area of the bottom surface and ε the ''apparent'' vertical strain during the compression, which is determined by the vertical displacement applied to the top surface. Comparison of the scaffold stiffness with the bone stiffness gives a measure for the relative deformation of the scaffold and for the amount of stress shielding that can be expected in the bone surrounding the scaffold.

(2) The histogram of the highest principal strains (compression or tension) over all the elements in the model is calculated. This is a measure for the activation of the osteoblasts grown inside the scaffold. If the scaffold and the bone have a comparable histogram, one can expect the osteoblasts in the scaffold to be activated in the same way as if they were inside real bone. When subjecting the scaffold to a physiological load, the strain distribution should be such that the majority of the osteoblasts feel a strain that activates bone formation. This means optimally a strain between 1500 and 4000 μstrain [5].

If these scaffold parameters are not satisfactory a redesign of the structure might be considered. Fig. 1 demonstrates the complete scaffold design process.

3. Results

The feasibility of the design process explained in this paper was demonstrated by applying it to an imaginary skeletal defect: a cylindrical bone sample had to be

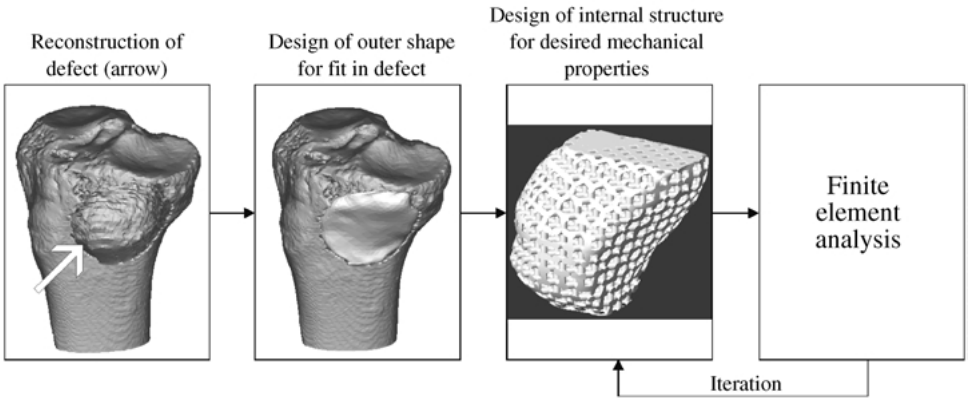

Figure 1 Design of the outer shape and internal architecture of the scaffold.

replaced by a biomimetic scaffold made of PMMA. A cylindrical bone sample, diameter 8 mm, height 10 mm was scanned using a microcomputed tomography system (Skyscan 1072, Skyscan b.v.b.a., Aartselaar, Belgium) with a pixel size of 20 μm. The bone sample was cancellous bone taken from a proximal human femur. Due to computational limitations only the central 4 mm in height of the bone sample could be modeled, and the images had to be resampled to a pixel size of 80 μm. After segmentation, each ''bone'' voxel was converted in a cube-shaped linear element of 80 μm side length. The resulting model can be seen in Fig. 2 (left).

An artificial structure with the same overall dimensions was created (cylinder, diameter 8 mm, height 4 mm). The structure consisted of a lattice made up of small intersecting beams of 250 × 250 μm cross-section, intersecting each other in three orthogonal directions. The geometry was meshed with cube-shaped quadratic elements of 250 μm side length. The resulting model is displayed in Fig. 2 (right). Table I shows the number of nodes and elements in both models.

On both models a compression with an ''apparent'' strain of -4000 μstrain in the vertical direction, the direction of the axis of the cylinder, was simulated. For a model height of 4 mm this corresponded to a vertical displacement of the top surface of the model over $4000 \times 10^{-6} \times 4\,\text{mm} = 0.016\,\text{mm}$.

Table II shows the assigned material properties, the porosity of both structures, the total reaction force at the bottom surface and the calculated apparent stiffness. Two materials have been assigned for the scaffold model: the biomaterial PMMA with an elastic modulus (E-modulus) of 3 GPa, and a ''theoretical'' material with an E-modulus of 12.517 GPa. The reason for this will be explained in the discussion. Both models have an identical geometry and mesh. Fig. 3 shows the calculated histograms of the principal strains for all elements in the bone model, the PMMA scaffold model and the theoretical scaffold model.

TABLE I Model size for bone model and scaffold model

	Number of nodes	Number of elements
Bone	138 610	80 931
Scaffold	39 809	3874

4. Discussion

Limited computational capacity allowed modeling of only 4 mm in height of the trabecular bone sample with a voxel size of 80 μm. According to Ulrich *et al*. [9] a hexahedral element size of 80 μm allows accurate trabecular bone modelling. An and Draughn [10] claim that, for mechanical compression testing of trabecular bone, cylindrical samples should have at least a diameter of 5 mm and a height/diameter ratio between 1 and 2. This means that the model should have a height between 8 mm and 16 mm. However, the goal of the experiment presented here was only to demonstrate the design principles. As computational power increases, larger samples can be analyzed, thus allowing the assessment of more reliable results.

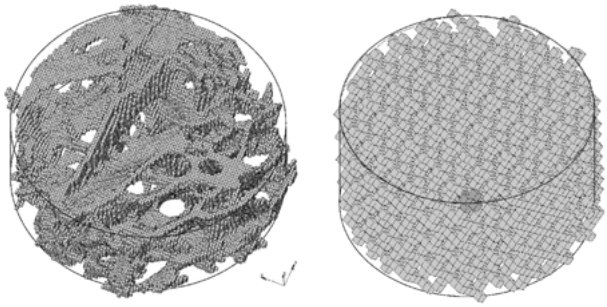

Figure 2 Finite element model of bone sample (left) and scaffold (right).

TABLE II Model properties, reaction forces and calculated apparent stiffness of bone, PMMA scaffold and theoretical scaffold

	Bone model	PMMA scaffold	Theoretical scaffold
Material properties (E-mod)	Bone tissue (10 GPa)	PMMA (3 GPa)	(12.517 GPa)
Porosity	79.4%	74.0%	74.0%
Reaction forces	170 N	41.9 N	171 N
Apparent stiffness	847 MPa	194 MPa	850 MPa

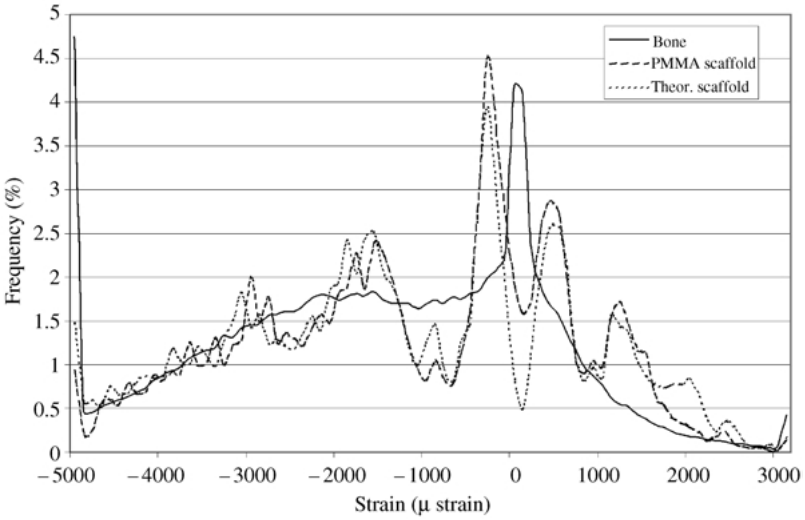

Figure 3 Histogram of principle strains in bone model, PMMA scaffold model and theoretical scaffold model.

The comparison of the strain histograms (Fig. 3) shows a good correspondence between the bone model and the scaffold models. This means that the osteoblasts seeded in the scaffold will probably be stimulated by mechanical strains that show a good resemblance to those of the bone sample. The apparent stiffness shows that the structure made of PMMA would be too soft to replace the bone sample. Possible changes could be to increase the cross section of the beams, or to use a stiffer material. Therefore a new E-modulus of a ''theoretical'' material was assigned to the scaffold and the compression test was repeated. The new E-modulus was calculated as:

$$E_{\text{theor}} = \frac{E^{\text{apparent}}_{\text{bone}}}{E^{\text{apparent}}_{\text{PMMA}}} \times E_{\text{PMMA}} = \frac{847}{194} \times 3\,\text{GPa} = 12.517\,\text{GPa}$$

As can be seen from Table II, the scaffold, made of the theoretical material, has an apparent stiffness that is very close to that of bone. As shown in Fig. 3 the histogram of the principal strains is deviating slightly from that of PMMA, but still has a good correspondence to bone. So given the proposed architecture for the scaffold, a material with the ''theoretical'' E-modulus would provide an excellent bone scaffold.

By taking images of the patient's bone, an implant is obtained that is personalized to the patient and to the location of the defect. Here μCT images of the bone sample are used, but for *in vivo* applications pQCT images or μMRI images can be used.

What is presented in this paper is a ''modus operandi'' for the biomechanical design of a personalized, biomimetic bone scaffold: an implant with an optimized geometry for a good fit in the defect, and the appropriate mechanical properties both for the load bearing function as well as for a good stimulation of new bone formation through activation of the osteoblasts. Here the highest principal strains (compression or tension) were used as a measure for osteoblast activation. However, if desired other parameters could be used for this purpose. For example the histogram of the strain energy density (SED) over all elements in each model can be calculated and compared. Also in a next step other parameters can be included in the design process to improve the biomimetic abilities of the scaffold. For example, the anisotropy of trabecular bone with its preferential orientation of the trabeculae can be taken into account.

Issues that still have to be solved are:

- Choice of material and production technique. Rapid prototyping techniques look promising since they allow the production of very complex architectures and provide an easy coupling to CAD [11].
- Transfer of the planning to the operating theater. Here we have the tools used in computer-assisted surgery (robot assistance, an optical guidance system, trial implant or surgical guide).
- Besides the outer geometry, internal architecture and mechanical properties also other properties of the scaffold are important (pore size, resorption rate) for the success of the implant.

In this paper, benign bone tumors were selected as a first application for the described design procedure. However, the procedure is also applicable to other bone defects. For example, in diaphyseal fractures where a large part of the diaphyseal bone is destroyed a bone scaffold can serve as an alternative for bone transport techniques (distraction osteogenesis). The scaffold can provide a temporary function restoration and at the same time stimulate new bone formation. In general the procedure is applicable where bone augmentation is needed at a load-bearing location.

5. Conclusion

Using the biomimetic approach explained in this paper a bone scaffold can be designed for the repair of skeletal load-bearing defects. The scaffold has mechanical properties that are optimized for avoiding stress shielding in the surrounding bone, for load bearing capacity, and for osteoblast activation.

Acknowledgment

This research was funded by the Belgian Prodex Agency.

References

1. S. GITELIS and D. J. MCDONALD, in ''Surgery for Bone and Soft-Tissue Tumors'', edited by M. A. Simon and D. Springfield (Lippincott-Raven Publishers, Philadelphia, 1998) p. 133–157.
2. S. GITELIS and D. J. MCDONALD, in ''Surgery for Bone and Soft-Tissue Tumors'', edited by M. A. Simon and D. Springfield (Lippincott-Raven Publishers, Philadelphia, 1998) p. 159–165.
3. M. KELLOMÄKI, H. NIIRANEN, K. PUURMANEN, N. ASHAMMAKHI, T. WARIS and P. TÖRMÄLÄ, *Biomaterials* **21** (2000) 2495–2505.
4. T. THOMAS, L. VICO, T. M. SKERRY, F. CAULIN, L. E. LANYON, C. ALEXANDRE and M. H. LAFAGE, *J. Appl. Physiol*. **80**(1) (1996) 198–202.
5. R. L. DUNCAN and C. H. TURNER, *Calcif. Tissue Int*. **57** (1995) 344–358.
6. R. MÜLLER, in ''Computer Technology in Biomaterials Science and Engineering'', edited by J. Vander Sloten (John Wiley & Sons Ltd, Chichester, 2000) p. 20–44.
7. B. VAN RIETBERGEN, S. MAJUMDAR, D. NEWITT and B. MACDONALD, *Clin. Biomater*. **17** (2002) 81–88.
8. S. J. HOLLISTER, R. A. LEVY, T. M. CHU, J. W. HALLORAN and S. E. FEINBERG, *Int. J. Oral Maxillofac. Surg*. **29(1)** (2000) 67–71.
9. D. ULRICH, B. VAN RIETBERGEN, H. WEINANS and P. RÜEGSEGGER, *J. Biomech*. **31** (1998) 1187–1192.
10. Y. H. AN and R. A. DRAUGHN, in ''Mechanical testing of bone and the bone-implant interface'' (CRC Press LLC, 2000) p. 181.
11. I. ZEIN, D. W. HUTMACHER, K. CHENG TAN and S. HIN TEOH, *Biomaterials* **23** (2002) 1169–1185.

Received 24 May
and accepted 29 May 2002